Hierarchical Cascade Controller for Assistance Modulation in a Soft Wearable Arm Exoskeleton

Binh Khanh Dinh, Michele Xiloyannis, Chris Wilson Antuvan, Leonardo Cappello, and Lorenzo Masia

Abstract—In recent years soft wearable exoskeletons, commonly referred to as exosuits, have been widely exploited in human assistance. Hence, a shared approach for a systematic and exhaustive control architecture is extremely important. Most of the exosuits developed so far employ a bowden cable transmission to conveniently place the actuator away from the end-effector. While having many advantages this actuation strategy presents some intrinsic limitations caused by the presence of nonlinearities, such as friction and backlash of the cables, which make it difficult to predict and control the dynamics between the device and the user. In this letter, we propose a novel hierarchical control paradigm for a cable-driven upper limb exosuits that aims at evaluating and consequently deliver the appropriate assistive torque to the user's elbow joint. The proposed control method comprises three main layers: an active impedance control which estimates the user's arm motion intention and guarantees an intuitive response of the suit to the wearer's motion; a mid-level controller which compensates for the backlash in the transmission and converts the reference arm motion to the desired position of the actuator; a low-level controller which is responsible for driving the actuation stage by compensating for the nonlinear dynamics occurring in the bowden cable to provide the desired assistive torque at the joint. Tests on healthy subjects show that wearing the exosuit reduces by 48.3% the muscular effort required to lift 1 kg and that the controller is able to modulate its level of assistance to the wearer's motor ability.

Index Terms—Prosthetics and exoskeletons, physically assistive devices, robust/adaptive control of robotic systems.

I. INTRODUCTION

THE introduction of compliant elements in robotics revolutionised the path to the design of applications with human in the loop: series elastic actuation [1] was the ignition to this new approach which has been widely accepted by a large part of the robotic community.

Compliant actuation opened a new scenario, alternative to the classic robotics precept "stiffer is better"; a new control approach was adopted with the purpose of transforming the force problem into a position problem where the deformation of the compliant element was the main indicator of the interaction forces between the human being and robotic device. Despite the large diffusion there are still several drawbacks which are far from being solved, especially in assistive technology. The aforementioned improvements in actuation and control solutions did not prevent the majority of exoskeletons from employing rigid components in parallel with the human biomechanics, resulting in ergonomics and usability which are still far from being optimal. Furthermore the weight of most of the rigid devices requires unacceptable metabolic costs from the wearer, resulting from movement restrictions and unwanted torques on the human joints [2].

Soft wearable exoskeletons (or exosuit) are the successive step to the introduction of compliant actuation, where not only the actuators but also the structure of the exoskeleton itself is designed to be compliant. Whilst not being suitable for applications requiring large forces and torques where rigid exoskeletons still show higher performance, exosuits' intrinsic compliance, portability and low-power consumption make them ideal for augmenting muscular strength or providing additional support in activities of daily living such as walking [3] and hand grasping [4], [5].

Exosuits allow to overcome the limitations introduced by conventional exoskeletons where the lack of mechanical compliance in the kinematic structure represents their major limiting factor. As an alternative to the stiff links of conventional exoskeletons, the exosuit design comprises fabrics and metamaterials to connect the human limb to the actuation stage, while the support is provided by the human musculoskeletal system. While for rigid exoskeletons the most used control approach was based on joint level torque assistance, where the actuation was located at the joint level, for exosuits this approach fails. A model-based controller on individual skeletal muscles is considered more appropriate and descriptive of the dynamic interaction between the exosuit and the human biomechanics.

Assistance of upper limbs especially is a challenging task since multiple actions might correspond to multiple controller layers that must account for the dynamic nature of human tasks, ranging from fine manipulation to weight/force compensation, to general interaction with the external environment and unpredictable dynamics. Last but not least the complexity of the

upper limb biomechanics is not confined to one plane [6], as for the walking gesture, but may involve multiple joints across multiple task dimensions.

One of the most significant examples of upper limb exosuit, which employed a fine model based controller implementation, was from Ueda *et al.* [7]. The novelty of the design was in the integrated human-exoskeleton model used to compute the interaction between the human muscle forces and torques generated by the exosuit. Assistance was evaluated by an embedded musculoskeletal model which calculated moment-arms from each of the muscles attached to the bones considering a total 51 muscles, while a kinematic model of the exoskeleton that consists of pneumatic actuators and supporting frames was integrated with the human model.

Despite the potentials and the demonstrated efficacy of the proposed computational approach via physiology-based criterion functions, the use of this method on impaired subjects showing a non stereotypical muscular activity is still under debate. That's why other examples of upper limb exosuits are extremely focused on helping subjects in replicating specific motor functions, involving only a limited number of joints and relying on controllers which, in order to preserve robustness, are highly task-specialized. Common strategies for intention detection are the use of biosignals (i.e. electromyography EMG), force trigger detection and proportional control to drive the devices and providing assistance.

An example of exosuit triggering assistance by EMG detection is from Delph *et al.* [8] for a cable-driven exosuit for hand and elbow assistance, where the fingers and the arm could be independently actuated using position of force control via surface EMG feedback. Other examples of wearable textile-garment based exosuits for hand rehabilitation come from Lee *et al.* [9] and In *et al.* [4], where an exo-tendon device and exo-glove respectively, used cable actuation to promote the recovery of fingers coordination and restoring functional hand movement after stroke or spinal chord injury. The two devices used different approaches: the exo-tendon was designed to be a rehabilitation device for clinical therapy, where the geometry and the disposition of the tendons, driven by seven motors, aimed at finely replicating different hand gestures (i.e. grasping, lateral grip, pinching etc.) by passive motion paradigm; the exo-glove relied on a more compact design, employing an underactuated mechanism and focusing its strength on the portability and versatility, where assistance was triggered by wrist motion.

The global scenario depicts two main approaches for controlling exosuits: the first on EMG-driven criteria functions with the intent of interpreting as accurately as possible the user intention and a second approach which is focused on control robustness and thus simplifies the number of functions that can be accomplished. If on one side the former approach is limited by the accuracy of the EMG signals and highly sensitive to subject specificity, the latter allows the user to replicate only predetermined specific actions.

An intention estimator and hierarchical control approach was proposed by Tsukahara *et al.* [10] to predict not only the motion intention but also the leg's swing speed for gait support in a rigid lower limb exoskeleton. This solution showed its advan-
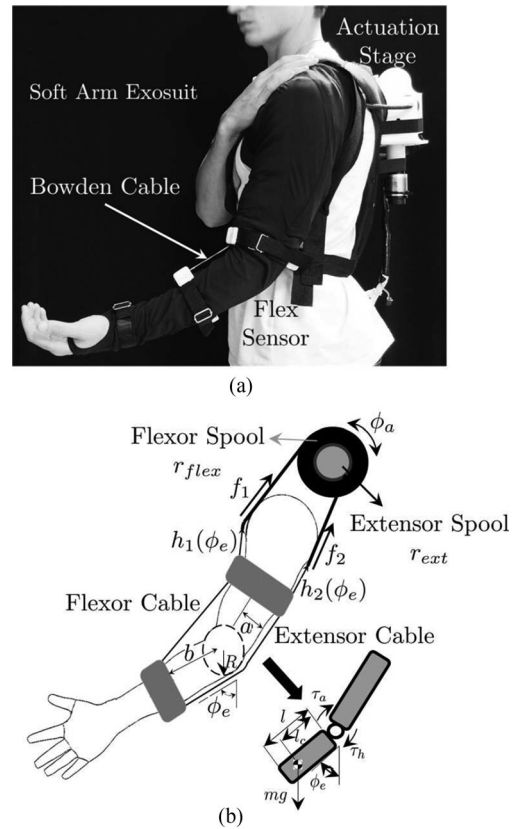

Fig. 1. (A): The soft arm exosuit with the bowden-cable transmission worn by the user; the actuation stage comprising the DC motor and the spool routing the cables on the user's back. (B): Human arm model.

tage compared to the voluntary intention using EMG and force trigger methods, adjusting the swing leg at optimal speed during walking. Thus this concept can be extended and applied to control soft exosuit devices.

The scope of the current letter is to implement a new control paradigm which allows to operate a soft arm exosuit providing assistance to the wearer's elbow flexion/extension. The proposed controller is referred to be "hierarchical" because it consists of three separate layers in cascade. Differently from previous contributions in literature, we aim at considering all the aspects ranging from human intention detection for assistance evaluation (high layer), to adaptive compensation of unwanted effects arising from the presence of nonlinear behaviours in the exosuit (mid and low layers) [11], [12]. The proposed hierarchical control architecture for wearable exosuit is tested for performance in trajectory following, and stability during assistance modulation is quantified and compared on healthy subjects.

II. CONTROLLER DESIGN

The hierarchical controller has been designed to work on the exosuit [13] shown in Fig. 1(A) consisting of a wearable garment which comprises a tendon driven transmission to mobilize the elbow in both flexion and extension. The actuation includes a traditional electromechanical DC motor and a planetary gear
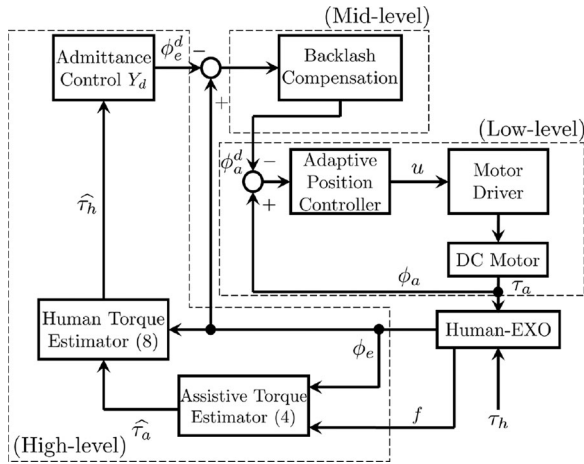
Fig. 2.   The control architecture consists in several blocks devoted to different tasks: from model-based admittance control (high-level), to compensation of nonlinear behaviour (i.e. backlash and friction) and desired trajectory tracking (mid and low-level).

mechanism with a reduction of 5:1 that moves a spool around which the cables, driving the elbow movements, are wrapped. The bending angle of the elbow joint ϕ_e can be monitored using a flex sensor embedded in the sleeve while two load cells are attached at the rigid braces to measure the cable tensions.

The controller has been designed in order to have a hierarchical structure starting from the evaluation of the level of assistance requested by the user and ending to the amount motion delivered to the joint throughout the tendon transmission. The control architecture shown in Fig. 2 comprises three layers: a *high-level*, a *mid-level* and a *low-level* controller. The objective of the high-level controller is to evaluate the amount of assistive torque $\widehat{\tau}_a$ requested by the user and consequently provide an active reference motion for the elbow ϕ_e^d. In the mid-level controller, backlash compensation translates the user's motion intention to the desired actuator motion ϕ_a^d, while the low-level controller is devoted to accurately track the motion reference. The inherent backlash caused by the cable slack in the bowden sheath introduces significant time delay and inaccuracy in joint position tracking. Hence, in the absence of a transmission mode that accounts for that nonlinear behaviour, control performances are extremely poor. Finally, the desired motion for the actuation stage is passed to the low-level controller, which computes the control signal u and sends it to the DC motor, to improve the tracking precision effectively, compensate the friction and provide assistance torque τ_a to the human-exosuit system. The designs for three control layers are described in detail in the following subsections.

A. Sensors Calibration

The flex sensor (Spectrasymbol, USA, accuracy $\pm 1°$) acts like a variable resistor whose output voltage is changed by flexing it. We used a simple voltage divider to convert a change in resistance into a change in voltage. The relationship between the output voltage and the bending angle ϕ_e was assumed to be linear [14]. A calibration step was necessary before the exper-

iment to render the measurement, obtaining a linear regression model to map the measured voltage to the angle ϕ_e. A similar calibration was applied to the load cell (Futek, USA), relating the voltage as a linear function of the force/cable tension. These procedures were repeated for each subject at the beginning of each experiment.

In order to filter the sensor noise, the measured angular position ϕ_e was low-pass filtered by a Butterworth second order filter with a cut-off frequency of 8Hz, then double differentiated to estimate the angular velocity $\dot{\phi}_e$ and acceleration $\ddot{\phi}_e$. These two signals were again smoothed using the same Butterworth filter.

B. High-Level Controller: Subject Assistance Evaluation

1) Assistive Torque Estimator: The intrinsic compliance of the exosuit does not allow to estimate the torque generated by the actuation unit by classical robotic approach. We used a mathematical model for bowden-cable transmission which provides an acceptable estimation of the torque, from the cable tensions [15] measured by load cells attached in the rigid braces. Fig. 1(B) shows the human arm model depicting the cable routing and a descriptive extension function $h_i(\phi_e)$ mapping the cables (flexor and extensor) displacement to the joint angle ϕ_e. The flexor cable has an extension function $h_1(\phi_e)$ defined as:

$$h_1(\phi_e) = 2\sqrt{a^2 + b^2} \cos\left(\tan^{-1}\left(\frac{a}{b}\right) + \frac{\phi_e}{2}\right) - 2b \quad (1)$$

while the extensor cable is described by:

$$h_2(\phi_e) = R\phi_e \quad (2)$$

where a is half of the width of the arm, b is the distance from the joint centre of rotation to the anchor points (rigid braces), and R is the radius of the elbow joint. ϕ_e is the bending angle of the elbow joint, referencing the forearm to the upper arm which is assumed to be vertical and aligned with gravity.

From the two extension functions $h_i(\phi_e)$ we can compute the relationship between the cable tensions f_i, recorded by the load cells and the torque $\widehat{\tau}_a$ delivered to the elbow joint. By defining the matrix J as:

$$J(\phi_e) = \frac{\partial h^T}{\partial \phi_e}(\phi_e) \quad (3)$$

where $h = \begin{bmatrix} h_1(\phi_e) & h_2(\phi_e) \end{bmatrix}^T$ represents the vector of cable extensions, the estimated assistive torque generated by bowden-cable transmission $\widehat{\tau}_a$ is expressed by the equation:

$$\widehat{\tau}_a = J(\phi_e)f \quad (4)$$

where $f = \begin{bmatrix} f_1 & f_2 \end{bmatrix}^T$ represents the vector of the measured cable tensions obtained by the two load cells.

2) Human Arm Model and Admittance Control: The human arm dynamics can be obtained by the Lagrangian formulation [16], by defining the kinetic K and the potential P energies of the arm as follows:

$$K = \frac{1}{3}ml^2\dot{\phi}_e^{\,2} \quad (5)$$

$$P = mgl_c(1 - \cos\phi_e) \quad (6)$$

where the forearm can be assumed to be a uniformly distributed mass m, with a total length l and a distance from the joint to the center of gravity (COG) l_c as shown in Fig. 1(B).

By defining the Lagrangian equation: $L = K - P$ and introducing a damping force for elbow opposing to the elbow motion, a simplified dynamic model of the human arm can be expressed as follow:

$$\tau = \tau_h + \tau_a = \frac{2}{3}ml^2\ddot{\phi}_e + b_e\dot{\phi}_e + mgl_c\sin\phi_e \qquad (7)$$

where τ is the resulting torque of the human action τ_h and the assistive torque from the exosuit τ_a, b_e is the viscous damping constant, and $g = 9.81\mathrm{m/s^2}$ represents the gravity constant.

The estimated torque deriving from the human muscles $\widehat{\tau_h}$ can be obtained from the inverse dynamic model expressed by (7), i.e.,

$$\widehat{\tau_h} = I_e\ddot{\phi}_e + b_e\dot{\phi}_e + mgl_c\sin\phi_e - \widehat{\tau_a} \qquad (8)$$

where $\widehat{\tau_a}$ is the estimated assistive torque obtained from (4), and $I_e = \frac{2}{3}ml^2$ represents the inertia of the elbow joint.

The parameters of (8) can be empirically measured and opportunely tuned on each individual subject following the simple known rules listed below [17]:

1) The forearm mass m as 2.2% of the total body weight M, i.e., $m = 0.022M\,[\mathrm{kg}]$
2) The length l_c from the elbow joint to the center of gravity as 68.2% of the total forearm length l, i.e., $l_c = 0.682l\,[\mathrm{m}]$
3) The human elbow viscous damping coefficient b_e can be tuned according to the damping ratio ξ: $b_e = 2I_e\Omega_0\xi$ where $\Omega_0 = \sqrt{\frac{mgl_c}{I_e}}$ is the resonance frequency. In this work, we chose $\xi = 1.2$, ensuring a stable and overdamped dynamic behaviour.

The exosuit which was used in the present letter has been conceived as a device to provide assistance to impaired people, in particular to stroke subjects who do not preserve enough residual voluntary capacity of motion to lift their elbow. Hence after the human torque $\widehat{\tau_h}$ has been estimated by the aforementioned model, a successive block in the controller must generate a reference trajectory ϕ_e^d which the actuation stage must deliver to the human joint. In order to provide a smooth intervention of the actuation on the user, an admittance controller has been used. The admittance controller has the role of changing the overall dynamics, increasing the transparency of the exosuit itself and decreasing the mechanical impedance of the human arm. The result is an assistance which is gradually modulated and depends on the mutual interaction between the device and the wearer. The admittance control block can be defined as follows:

$$I_e^d\ddot{\phi}_e^d + b_e^d\dot{\phi}_e^d + K_e^d\sin\phi_e^d = \widehat{\tau_h} \qquad (9)$$

where I_e^d, b_e^d, and K_e^d denotes the desired inertia, viscous damping and gravitational torque acting at the elbow joint, respectively, while and $\widehat{\tau_h}$ represents the estimated human torque obtained from (8).

It can be noticed that in order to reduce the provided assistance $\widehat{\tau_h}$, the admittance controller must be tuned in such a way that the desired impedance is lower than the real one from the human arm [18] (i.e. $I_e^d \leq I_e$, $b_e^d \leq b_e$, and $K_e^d \leq mgl_c$). In this
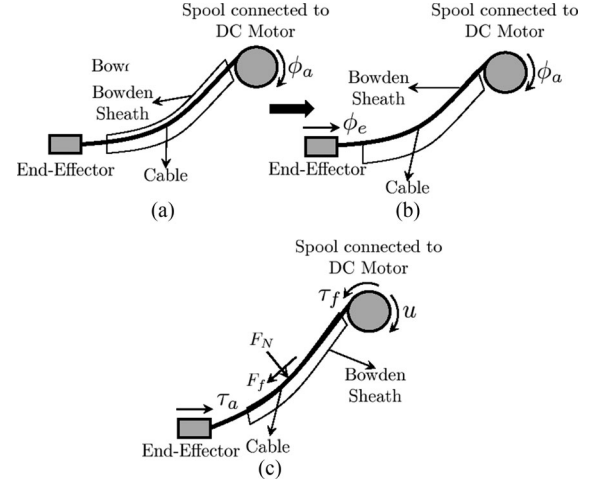

Fig. 3. (A): Backlash caused by cable slack in the bowden sheath. (B): Under tension, the motion is transmitted from extension to flexion and vice versa. (C): Varying friction F_f occurring when the cable slides along the inner wall of the bowden sheath resulting in the lost in assistive torque τ_a.

study, we want to verify how the exosuit can assist its wearer in a gravity compensation paradigm. The desired gains of the admittance controller (I_e^d, b_e^d, and K_e^d) were chosen based on the actual human elbow joint dynamics defined in (10), and the level of assistance is regulated by a factor α ($0 < \alpha \leq 1$) which multiples the gravity compensation factor K_e^d. With such selection, the dynamics of the admittance controller can be proven to be stable and overdamped

$$\begin{cases} I_e^d = I_e = \frac{2}{3}ml^2 \\ b_e^d = b_e = 2I_e\Omega_0\xi \\ K_e^d = \alpha mgl_c \\ \alpha = \alpha_0\tanh\left(\frac{\dot{\phi}_e}{\epsilon_\alpha}\right) + \alpha_1 \end{cases} \qquad (10)$$

where α_0 and α_1 are two constants experimentally chosen to bound the intervention of the assistance; ϵ_α denotes the sensitivity coefficient of the hyperbolic function $\tanh(.)$. The factor α increases with the measured joint velocity $\dot{\phi}_e$, meaning that the level of assistance is strictly dependent on the user's residual motion capacity: a high motion speed from the user (i.e. high motor ability) corresponds to a low assistive torque provided by the exosuit and vice versa, and the device is therefore able to gradually tune the assistive torque based on the a real-time estimation of the subject's capacity of motion.

C. Mid-level Controller: Adaptive Backlash Compensation

The purpose of the mid-level control layer is to compensate for a specific non linear behaviour, intrinsic in the cable driven mechanisms. The desired angular motion ϕ_e^d from the admittance control block must be converted into a motion ϕ_a^d which is successively sent to the servomotor and delivered at the elbow joint. The mid-level controller is implemented with the purpose to specifically compensate for backlash phenomena. Fig. 3(A)–(B) shows a conceptual representation of backlash caused by the cable looseness in the bowden sheath: since the backlash effect is unpredictable and continuously changes during the system's

operation due to variability of the geometry of the flexible bowden sheath, we implemented a nonlinear adaptive controller [19] updating the backlash model during each iteration of the controller. The relationship between the desired motion ϕ_e^d and the motion the actuation unit ϕ_a^d is defined adopting the Bouc-Wen hysteresis model [20], such that the desired elbow motion is a function of the actuator rotation and of a term representing the backlash uncertainties:

$$\phi_e^d = \alpha_\phi \phi_a^d + D \rightarrow \beta \phi_e^d = \phi_a^d + \beta D \qquad (11)$$

where α_ϕ represents the positive ratio of ϕ_e^d to ϕ_a^d; $\beta = \frac{1}{\alpha_\phi}$ is the inverse of α_ϕ; and D represents the model uncertainties due to the bowden sheath's configuration variations during operation. It can be assumed that: $|D| \leq D_m$ where D_m denotes a bounded value of D.

The adaptive controller design uses a reference motion ϕ_e^r and filtered tracking error s as in:

$$\begin{cases} e = \phi_e - \phi_e^d \\ s = \lambda e + \int_0^t e d\tau \rightarrow \dot{s} = \lambda \dot{e} + e \\ \phi_e^r = \phi_e^d - \lambda \dot{e} \end{cases} \qquad (12)$$

where e represents the tracking error between the desired elbow joint motion ϕ_e^d and the measured one ϕ_e; and λ is an arbitrarily positive constant.

Since the elbow joint is supposed to follow a given trajectory ϕ_e^d, the desired actuator state ϕ_a^d can be chosen as:

$$\phi_a^d = \widehat{\beta}\left(\phi_e^r - \widehat{D_m}\tanh\left(\frac{s}{\epsilon}\right)\right) - \kappa s \qquad (13)$$

where $\widehat{\beta}$ and $\widehat{D_m}$ are the estimated value of β and D_m respectively (such notation will be used for all variables from now on); and κ, ϵ are positive constants.

Replacing ϕ_a^d from (13) to (11) leads to the dynamics of the variable s as:

$$\beta \dot{s} + \kappa s = \widetilde{\beta}\bar{\phi} - \beta\widetilde{D_m}\tanh\left(\frac{s}{\epsilon}\right) - \beta\left(D_m\tanh\left(\frac{s}{\epsilon}\right) - D\right) \qquad (14)$$

where $\bar{\phi} = \phi_e^r - \widehat{D_m}\tanh\left(\frac{s}{\epsilon}\right)$; $\widetilde{\beta} = \widehat{\beta} - \beta$ is the estimated error of β; and $\widetilde{D_m} = \widehat{D_m} - D_m$ is the estimated error of D_m.

Therefore, the adaptation law for backlash model parameters $\widehat{\beta}$ and $\widehat{D_m}$ is:

$$\begin{cases} \dot{\widehat{\beta}} = -\delta_1 \bar{\phi} s \\ \dot{\widehat{D_m}} = \delta_2 \beta \tanh\left(\frac{s}{\epsilon}\right) s \end{cases} \qquad (15)$$

where δ_1, δ_2 are positive adaptation gains. The initial values for $\widehat{\beta}$ and $\widehat{D_m}$ are set to be zero.

D. Low-Level Controller: Adaptive Friction Compensation and Position Control

The low level control layer is intended to drive the actuation stage by sending the input to the DC motor and to compensate for the nonlinear friction occurring because of the cable sliding along the bowden sheath (Fig. 3(C)). The friction continuously and unpredictably changes according to the curvature of the sheath which moves with the subject arm motion; if

not compensated, the torque generated by the actuator is partly lost during operation. An adaptive algorithm compensates for the friction and controls the DC motor in tracking the desired trajectory ϕ_a^d. From Fig. 3(C) the actuator with the friction is modelled as follows:

$$J\ddot{\phi}_a + B\dot{\phi}_a + \tau_f = u \qquad (16)$$

where J and B represent the inertia and damping coefficient of the actuation stage, τ_f the friction torque, and u is the control output to be sent to the DC motor. The dynamic parameters of the actuation stage comprising the DC motor and the bowden cable and the friction variability are unknown: the LuGre model for the dynamic friction compensation [21], allows to express τ_f as follows:

$$\tau_f = B_v \dot{\phi}_a + \tau_z\left(\phi_a, \dot{\phi}_a, z\right) \qquad (17)$$

where z is a variable in the Lugre model; $B_v\phi_a$ represents the viscous friction; and $\tau_z\left(\phi_a, \dot{\phi}_a, z\right)$ represents the dynamic friction depending on z. It is assumed that τ_z to be bounded by: $\left|\tau_z\left(\phi_a, \dot{\phi}_a, z\right)\right| \leq \tau_{zm}$.

Before designing the control signal u, we define the tracking error e_1, reference motion ϕ_a^r and filtered tracking error s_1 for the actuator as:

$$\begin{cases} e_1 = \phi_a - \phi_a^d \\ s_1 = \dot{e}_1 + \lambda_1 e_1 \\ \phi_a^r = \dot{\phi}_a^d - \lambda_1 e_1 \end{cases} \qquad (18)$$

where ϕ_a and ϕ_a^d denote the measured and desired rotation of the DC motor, respectively; and λ_1 is an arbitrary positive constant.

The control signal u for the DC motor is designed as:

$$u = \widehat{J}\ddot{\phi}_a^r + \left(\widehat{B} + \widehat{B_v}\right)\dot{\phi}_a - \widehat{\tau_{zm}}\tanh\left(\frac{s_1}{\epsilon_1}\right) - \kappa_1 s_1 \qquad (19)$$

where $\widehat{J}$ is the estimated value of J; $\widehat{B}$ and $\widehat{B_v}$ denote respectively the estimated values of B and B_v; $\widehat{\tau_{zm}}$ denotes the estimated value of τ_{zm}; and ϵ_1 and κ_1 are two positive constants.

Substituting (17) and (19) to (16), and replacing $B_t = B + B_v$ result in the dynamics of the tracking error s_1 as:

$$J\dot{s}_1 + \kappa_1 s_1 = \widetilde{J}\ddot{\phi}_a^d + \widetilde{B_t}\dot{\phi}_a - \widetilde{\tau_{zm}}\tanh\left(\frac{s_1}{\epsilon_1}\right)$$
$$- \tau_{zm}\tanh\left(\frac{s_1}{\epsilon_1}\right) - \tau_z\left(\phi_a, \dot{\phi}_a, z\right) \qquad (20)$$

where $\widetilde{J} = \widehat{J} - J$ is the estimated error of J; $\widetilde{B_t} = \widehat{B_t} - B_t$ is the estimated error of B_t; and $\widetilde{\tau_{zm}} = \widehat{\tau_{zm}} - \tau_{zm}$ is the estimated error of τ_{zm}.

Therefore, the unknown parameters $\widehat{J}$, $\widehat{B_t}$, and $\widehat{\tau_{zm}}$ are updated at each period by:

$$\begin{cases} \dot{\widehat{J}} = -\delta_3 \ddot{\phi}_a^r s_1 \\ \dot{\widehat{B_t}} = -\delta_4 \dot{\phi}_a s_1 \\ \dot{\widehat{\tau_{zm}}} = \delta_5 \tanh\left(\frac{s_1}{\epsilon_1}\right) s_1 \end{cases} \qquad (21)$$

where δ_3, δ_4, and δ_5 are positive adaptation gains.

TABLE I
AVERAGE IDENTIFIED CONTROL MODEL PARAMETERS

Parameters	Values [Unit]
a, b, R	$0.05[\mathrm{m}], 0.10[\mathrm{m}], 0.06[\mathrm{m}]$
m, l	$1.55 \pm 0.12[\mathrm{kg}], 0.24 \pm 0.03[\mathrm{m}]$
l_c	$0.2 \pm 0.02[\mathrm{m}]$
b_e	$1.50[\mathrm{Nm}/(\mathrm{rad}/\mathrm{s})]$
$\alpha_0, \alpha_1, \epsilon_\alpha$	$0.5, 0.5, 0.1$
$\lambda, \kappa, \epsilon, \sigma_1, \sigma_2$	$2, 10, 0.01, 2, 2$
$\lambda_1, \kappa_1, \epsilon_1, \sigma_3, \sigma_4, \sigma_5$	$1.5, 5, 0.01, 1, 1, 1$

Fig. 4. The experiment was run by instructing the subjects to replicate the movements of a virtual avatar on the screen, trying to match the elbow speed.

III. EXPERIMENTAL EVALUATION

A. Experimental Protocol

The experiment was performed on a group of three healthy subjects (males, age: 26.6±1.5 years). They all provided written informed consents prior to the experiment, and the procedures were approved by the Institutional Review Board at Nanyang Technology University. The parameters of the subject's arm, the exosuit, and of the control scheme are shown in Table I and were obtained as described in Section II-B1 (mean ± standard deviation for m, l, l_c).

The experiment aims at demonstrating that the proposed hierarchical controller is accurate, stable and provides a smooth intervention when assistance is requested by the users, modulating the amount of torque at the elbow depending on the capacity of motion of the subject and decreasing the muscular effort during load manipulation. During the experiment the subjects were instructed to flex/extend their forearm, following the motion of a virtual avatar on a screen to match the range of motion and speed (as shown in Fig. 4) while holding a $1\mathrm{kg}$ load in their left hand, in two distinct task phases. The visual input was used as a way to standardize the velocity and amplitude of the movements across subjects, allowing across-subjects comparisons of muscular effort.
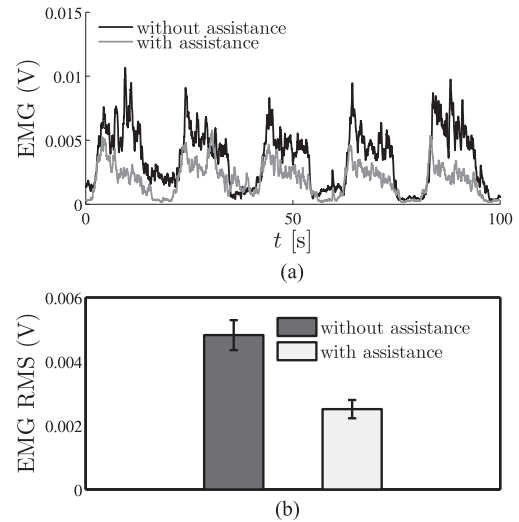

Fig. 5. (A) EMG amplitude comparison on a single subject with and without the exosuit's assistance. (B) Bar plot showing the mean and standard deviation of the RMS of the EMG activity, averaged over repetitions and subjects.
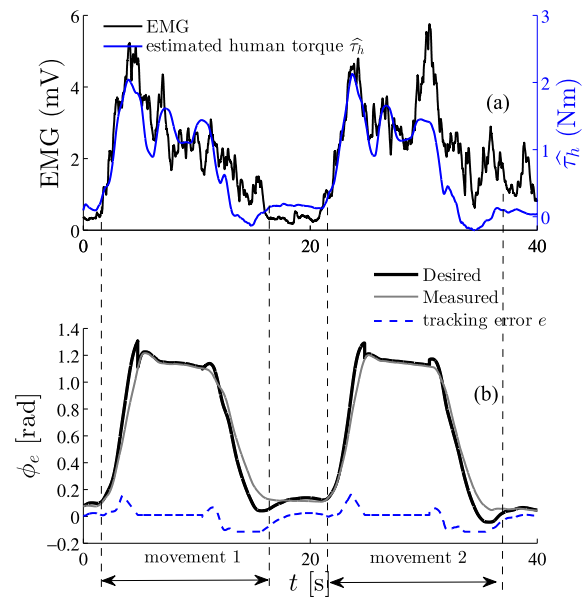

Fig. 6. EMG and estimated human torque and trajectory tracking accuracy. (A) Amplitude of the EMG signal (black) of a subject performing elbow flexion/extension tasks and estimated human torque (blue) as computed from (8). (B) Trajectory tracking accuracy ϕ_e^d and ϕ_e during two repetitive flexion/extension movements.

1) Performing 10 repetitive flexion/extension movements with and without assistance delivered by the exosuit to prove that the use of the proposed device/controller effectively decrease the muscular activity, helping the wearer to complete the task;

2) Performing 10 repetitive flexion/extension movements at two different speeds ($\dot{\phi}_e^1 = 0.3\mathrm{rad}/\mathrm{s}$ and $\dot{\phi}_e^2 = 0.6\mathrm{rad}/\mathrm{s}$), to show that the intervention of the exosuit is based on the subject's capacity of motion. It is commonly accepted that kinematics in stroke subjects are dramatically jeopar-
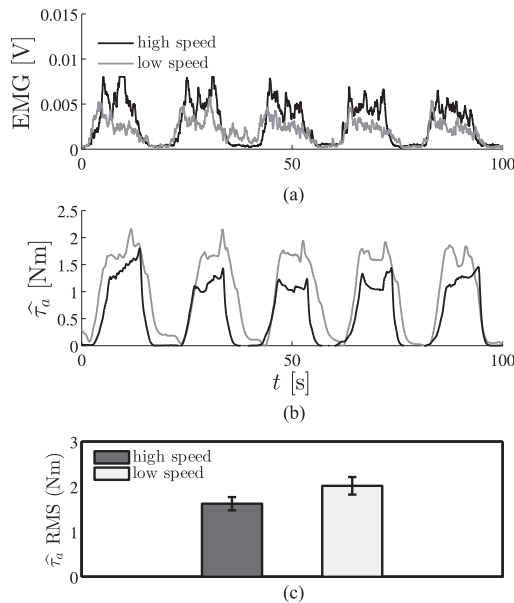
Fig. 7. Evaluation of the effectiveness of the assistance modulation at different elbow speeds. (A) The amplitude of the EMG activities are shown when a single subject performed the elbow motions at two different velocities. (B) The estimated assistive torques $\widehat{\tau}_a$ at low (light grey) and high (dark grey) elbow speed motions. (C) Bar plot showing the mean and standard deviation of the RMS of $\widehat{\tau}_a$, averaged over repetitions and subjects.

dized and a lower elbow speed is associated to a reduced voluntarily capacity of motion. For this reason, asking subjects to move at a lower and higher speed implies that the proposed controller should interpret a lower speed as a reduced motion capacity and consequently increase the level of assistive torque respectively, as described in the Section II-B1

Muscular effort was estimated from the Root Mean Square (RMS) of the EMG activity of the main muscle involved in performing elbow flexion movements, i.e. the biceps brachii of the left arm. The raw EMG was acquired using Trigno wireless EMG sensors (Delsys Inc.) and was pre-processed in Matlab Simulink using a full-wave rectification, followed by a low-pass second-order Butterworth filter with a 8Hz cut-off frequency. The elbow joint angle ϕ_e was acquired during the experiment and used for control purposes using the flex sensor. Data acquisition and motor control were performed using the Quanser Quarc real-time workstation running at 1kHz refresh rate.

B. Experimental Results

Results of the first task comparing the EMG activities of one subject with and without the assistance are depicted in Fig. 5(A), showing a clear decrease in the amplitude of the EMG activity when the exosuit was assisting the motion. Analysis of the RMS value of the EMG signal, averaged over repetitions and subjects, is shown in Fig. 5(B). The latter shows an average drop in RMS of 48.3% between the non-assisted and assisted case. Fig. 6(A) shows the estimated human torque $\widehat{\tau}_h$, as computed from (8) and the recorded EMG activities during two elbow flexion/extension tasks from one of the participants, it can be seen that the estimated human torque shows a similar curve as

the processed EMG signal. This results in an elbow trajectory profile ϕ_e as shown in Fig. 6(B), with the tracking error e ranging between $\pm 0.1\text{rad}$ and a fast response time.

The second experiment examines the efficacy of the controller in adapting its contribution to the user's capacity of motion. The subjects performed the elbow movement at two different angular velocities ($\dot{\phi}_e^1 = 0.3$ rad/s and $\dot{\phi}_e^2 = 0.6$ rad/s) and the exosuit modulates the degree of assistance, i.e. the estimated assistive torque $\widehat{\tau}_a$, based on the speed of the subjects. Fig. 7(A-B) shows the EMG activities and the delivered assistive torques $\widehat{\tau}_a$ respectively for one typical subject at the two execution speeds: it is observable that at lower speed (lower capacity of motion) the controller provides a higher assistive torque $\widehat{\tau}_a$ than when the subject moves at the higher speed (which corresponds to a higher capacity of motion). The same result was observed for the whole group of subjects. An analysis of the estimated assistive torque $\widehat{\tau}_a$ supports these results: Fig. 7(C) shows that the mean RMS value of the estimated assistive torque $\widehat{\tau}_a$, averaged over subjects and trials, is lower at a higher speed of motion, confirming that the controller has adapted to the lower motor ability of the subjects by providing higher assistance.

IV. DISCUSSION AND CONCLUSION

It has been almost three decades that robot aided rehabilitation and assistive robotics introduced the new concept of gentle human-robot interaction based on soft actuations and materials, yet many questions on ergonomic design and control implementation remain unanswered. For soft wearable exoskeletons, formulating an effective and robust control approach is of major importance. In the present letter we showed that appropriately designing a multi-layered controller, which takes into account the nonlinear behaviour of the exosuit's soft complaint nature, we can both reduce the muscle effort required for a simple lifting movement and adapt the level of assistance depending on the wearer's motor ability.

We introduced the problem of motion intention detection by formulating a model of the human arm which can be used to predict the human joint torque from only a simple load cell. An admittance controller was dedicated to increase the transparency of the device, while the nonlinear behaviours of the cable-driven transmission (i.e. backlash and friction) were opportunely compensated by means of adaptive mathematical models. The results have shown that the muscular effort of subjects using the exosuit and the associated controller is lower than performing action with no assistance, whilst a high-level of tracking accuracy is achieved. It is worth to highlight that the reduction of muscular activation was not provided by a predominant action of the device replacing entirely the human voluntary motion, but rather by a coordinated interaction between the exosuit and the user. In this study, we assumed that the upper arm was aligned with the direction of gravity and the forearm moved on the sagittal plane only, neglecting the shoulder movements. For the future work, the proposed hierarchical controller can be extended to assist the arm with shoulder flexion/extension by using a sensor (i.e. IMU) to measure the orientation of the upper arm with gravity, allowing to update the Lagrangian equation and controller

accordingly. In addition, a more comprehensive model of the elbow joint on the transverse plane, i.e. 90° shoulder abduction, can be defined such that the proposed controller can be applied to assist the arm horizontally.

We further showed that the proposed controller was able to tune the level of assistance depending on the voluntary motion capacity of the subjects. This strategy somewhat resembles the "assist-as-needed" paradigm [22], and to our knowledge it is the first time that this kind of approach is being formulated for a wearable exosuit rather than for end-effector robotics device. Keeping in mind that the users of assistive devices, who are mainly hemiplegic or impaired subjects, must rely very intimately on the exosuit which is attached to their bodies, and the "gentle intervention" from the controller represents a delicate and pivotal goal.

REFERENCES

[1] D. W. Robinson, "Design and analysis of series elasticity in closed-loop actuator force control," Ph.D. dissertation, Dept. Mechanical Eng., Massachusetts Inst. Technol., Cambridge, MA, USA, 2000.

[2] N. Jarrassé and G. Morel, " Connecting a human limb to an exoskeleton," *IEEE Trans. Robot.*, vol. 28, no. 3, pp. 697–709, Jun. 2012.

[3] A. T. Asbeck, K. Schmidt, and C. J. Walsh, "Soft exosuit for hip assistance," *Robot. Auton. Syst.*, vol. 73, pp. 102–110, 2015.

[4] H. In, B. B. Kang, M. Sin, and K. J. Cho, "Exo-glove: A wearable robot for the hand with a soft tendon routing system," *IEEE Robot. Autom. Mag.*, vol. 22, no. 1, pp. 97–105, Mar. 2015.

[5] M. Xiloyannis, L. Cappello, D. B. Khanh, S.-C. Yen, and L. Masia, "Modelling and design of a synergy-based actuator for a tendon-driven soft robotic glove," in *Proc. 6th IEEE Int. Conf. Biomed. Robot. Biomechatronics*, 2016, pp. 1213–1219.

[6] D. Bennett, J. M. Hollerbach, Y. Xu, and I. Hunter, "Time-varying stiffness of human elbow joint during cyclic voluntary movement," *Exp. Brain Res.*, vol. 88, no. 2, pp. 433–442, 1992.

[7] J. Ueda, M. Hyderabadwala, V. Krishnamoorthy, and M. Shinohara, "Motor task planning for neuromuscular function tests using an individual muscle control technique," in *Proc. IEEE Int. Conf. Rehabil. Robot.*, 2009, pp. 133–138.

[8] M. A. Delph, S. A. Fischer, P. W. Gauthier, C. H. M. Luna, E. A. Clancy, and G. S. Fischer, "A soft robotic exomusculature glove with integrated sEMG sensing for hand rehabilitation," in *Proc. IEEE Int. Conf. Rehabil. Robot.*, 2013, pp. 1–7.

[9] S. W. Lee, K. A. Landers, and H.-S. Park, "Development of a biomimetic hand exotendon device (biomhed) for restoration of functional hand movement post-stroke," *IEEE Trans. Neural Syst. Rehabil. Eng.*, vol. 22, no. 4, pp. 886–898, 2014.

[10] A. Tsukahara, Y. Hasegawa, K. Eguchi, and Y. Sankai, "Restoration of gait for spinal cord injury patients using hal with intention estimator for preferable swing speed," *IEEE Trans. Neural Syst. Rehabil. Eng.*, vol. 23, no. 2, pp. 308–318, 2015.

[11] T. N. Do, T. Tjahjowidodo, M. W. S. Lau, and S. J. Phee, "Adaptive control for enhancing tracking performances of flexible tendonsheath mechanism in natural orifice transluminal endoscopic surgery (notes)," *Mechatronics*, vol. 28, pp. 67–78, 2015.

[12] T. N. Do, T. Tjahjowidodo, M. W. S. Lau, and S. J. Phee, "Nonlinear friction modelling and compensation control of hysteresis phenomenon for a pair of tendon-sheath actuated surgical robots," *Mech. Syst. Signal Process.*, vol. 60–61, pp. 770–784, 2015.

[13] B. K. Dinh, L. Cappello, and L. Masia, "Localized extreme learning machine for online inverse dynamic model estimation in soft wearable exoskeleton," in *Proc. 6th IEEE Int. Conf. Biomed. Robot. Biomechatronics*, 2016, pp. 580–587.

[14] G. Saggio, F. Riillo, L. Sbernini, and L. R. Quitadamo, "Resistive flex sensors: A survey," *Smart Mater. Struct.*, vol. 25, no. 1, 2016, Art. no. 013001.

[15] R. M. Murray, Z. Li, S. S. Sastry, and S. S. Sastry, *A Mathematical Introduction to Robotic Manipulation* pp. 293–296, 1994.

[16] K. Kong and M. Tomizuka, "Control of exoskeletons inspired by fictitious gain in human model," *IEEE/ASME Trans. Mechatronics*, vol. 14, no. 6, pp. 689–698, Dec. 2009.

[17] M. B. Weinger, M. E. Wiklund, and D. J. Gardner-Bonneau, *Handbook of Human Factors in Medical Device Design*. Boca Raton, FL, USA: CRC Press, 2010.

[18] G. Aguirre-Ollinger, J. E. Colgate, M. A. Peshkin, and A. Goswami, "Active-impedance control of a lower-limb assistive exoskeleton," in *Proc. IEEE 10th Int. Conf. Rehabil. Robot.*, Jun. 2007, pp. 188–195.

[19] J.-J. E. Slotine *et al.*, *Applied Nonlinear Control*, vol. 199, no. 1. Englewood Cliffs, NJ, USA: Prentice-Hall, 1991.

[20] F. Ikhouane and J. Rodellar, *Systems With Hysteresis: Analysis, Identification and Control Using the Bouc-Wen Model*. New York, NY, USA: Wiley, 2007.

[21] H. Olsson, K. J. Aström, M. Gäfvert, C. Canudas De Wit, and P. Lischinsky, "Friction models and friction compensation," *Eur. J. Control*, vol. 4, no. 3, pp. 176–195, 1998.

[22] L. E. Kahn, P. S. Lum, W. Z. Rymer, and D. J. Reinkensmeyer, "Robot-assisted movement training for the stroke-impaired arm: Does it matter what the robot does?" *J. Rehabil. Res. Develop.*, vol. 43, no. 5, pp. 619–630, 2006.